# Optical processing by fringed speckles registered in a BSO crystal

**Myrian Tebaldi**
**Luciano Angel Toro***
**Marcelo Trivi**
**Néstor Bolognini**
Centro de Investigaciones Ópticas
CIOp (CONICET, CIC)
and
OPTIMO Dpto. de Fisicomatemática
Facultad de Ingeniería
UNLP Casilla de Correo 124
1900, La Plata, Argentina
E-mail: myrianc@odin.ciop.unlp.edu.ar

**Abstract.** An alternative image multiplexing technique, employing a multiple-aperture pupil for each exposure, is presented. The aperture arrangement of the pupil is modified between exposures. A thick photorefractive BSO crystal is used as recording material. The technique allows concentrating the spectral components of a pair of images selectively into isolated spots in the Fourier plane. Two applications are proposed, in image processing and optical metrology.  [S0091-3286(00)02712-4]

Subject terms: speckle; photorefractive crystal; multiplexing.

Paper 990453 received Nov. 15, 1999; revised manuscript received July 16, 2000; accepted for publication July 28, 2000.

## 1 Introduction

Several techniques have been proposed for image multiplexing in holography. In particular, Leith and Upatnieks[1] used different spatial carriers by employing a diffuser for different spatial signals. Caufield[2] suggested recording each wavefront on a spatially distinct area of the hologram, but allowing spatially distinct areas to occupy the full area of the hologram. Also, the angular selectivity of volume holograms has been exploited to increase the multiplexing capability. For this purpose, photorefractive media have been widely employed.[3]

Photorefractive crystals, in particular those of the sillenite family, combine real-time response, reversibility, and high sensitivity in the visible region of the spectrum, which make them very attractive for holography, optical data storage, and optical information processing.[4] In addition, crystals of the sillenite family have been found to be very attractive for real-time speckle applications.[5–10] The use of BSO crystals for recording and processing double-exposure speckle patterns has been demonstrated experimentally;[5,6] they are used instead of photographic plates, in conventional arrangements, for real-time and *in situ* measurement of displacements. Analysis of speckle-pattern movement is a well-known noncontact technique to measure displacements, deformations, tilts, and vibrations of real objects having optically rough surfaces.[11,12] In addition, the introduction of suitable spatial-frequency carriers, by internally modulating imaged speckles, allows concentrating the spectral content into spatially separated regions in the Fourier plane.[12]

In this paper, an alternative image multiplexing technique, employing a multiple-aperture pupil for each exposure, is outlined. The aperture arrangement of the pupil is modified between exposures. The use of different multiple-aperture pupils for recording each image has a definite advantage in that it allows concentrating the spectra components of individual or several speckled images selectively into isolated spots in the Fourier plane. A thick photorefractive BSO crystal is used as the recording material; its main advantages are its large information capacity, high diffraction efficiency, and real-time response.

In the next section we describe the recording and reconstruction processes. A registration procedure using four different pupil arrangements is presented. In the third section, applications to multiple storage using selected aperture pupils are analyzed.

Two possible applications are proposed for the use of multiple apertures in a multiple-exposure scheme. In image processing, a real-time binary OR operation between images is carried out. Another application consists in storing in the crystal the information belonging to several in-plane displacements. The possibility of employing different multiple-aperture pupils combined with the advantage of using a photorefractive medium is exploited to implement a quasi-real-time extension of speckle photography. The use of BSO crystal as the recording medium is appropriate for the applications proposed because it permits multiple storage in real time.

## 2 Multiplexing with Multiple Apertures

The experimental setup is shown in Fig. 1. An optically rough surface located in the $x$-$y$ plane is illuminated with a laser of wavelength $\lambda_W = 514\,\text{nm}$. This input is imaged onto a photorefractive BSO crystal. A multiple-aperture pupil mask $P^k$ is located immediately in front of the imaging lens $L_1$ in the $u$-$v$ plane. This mask consists of an arrangement of $q$ identical circular apertures $a_1^k, a_2^k, \ldots, a_q^k$. The distance between the lens and the crystal is $Z_C$, and the distance between the input and the lens is $Z_0$. A speckled image of the input is produced through each aperture of the pupil. The complex amplitudes of waves going through different apertures are statistically independent, because different components of the angular spectrum of the scattered light are accepted by them. Moreover, the resulting speckle pattern in the BSO crystal arises from the interference of speckle distributions produced by each aperture pair, be-

*Permanent address: Universidad EAFIT, Medellín, Colombia.

 

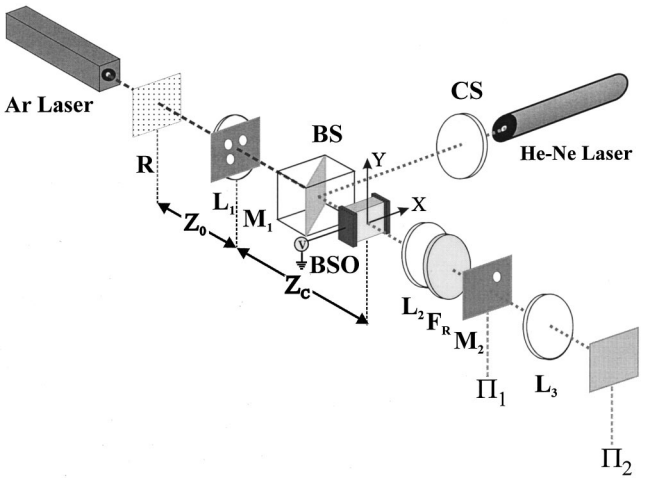


**Fig. 1** Experimental setup: R, random diffuser; $L_1$, $L_2$, and $L_3$, lenses; $M_1$, pupil mask; $M_2$, filtering mask; CS, collimator system; BS, beamsplitter; $F_R$, inteference filter ($\lambda = 633$ nm); $\Pi_1$, Fourier plane; $\Pi_2$, image plane.

cause they are coherent. In summary, in the crystal, the speckle pattern is modulated by a complex system of fringes existing in the whole volume of individual speckle grains.

Let $a_i^k$ and $a_j^k$ represent two apertures belonging to the pupil mask $\mathsf{P}^k$ associated with the $k$th exposure. The distance between the respective centers $(u_i^k, v_i^k)$ and $(u_j^k, v_j^k)$ of the apertures $a_i^k$ and $a_j^k$ $(1 \leq i \neq j \leq q)$ is $d_{ij}^k = [(u_j^k - u_i^k)^2 + (v_j^k - v_i^k)^2]^{1/2}$, and the line that joins them forms an angle $\alpha_{ij}^k = \tan^{-1}[(v_j^k - v_i^k)/(u_j^k - u_i^k)]$ with the $u$ axis. Taking into account this definition, each elementary fringe system $f_{ij}^k$ in the imaged speckles has a spatial period $p_{ij}^k = Z_C \lambda_W / d_{ij}^k$, and its orientation is given by $\alpha_{ij}^k$. The direction of each fringe system can be described by the versor $\hat{\mathbf{f}}_{ij}^k = (\cos \alpha_{ij}^k)\hat{\mathbf{u}} + (\sin \alpha_{ij}^k)\hat{\mathbf{v}}$, where $\hat{\mathbf{u}}$ and $\hat{\mathbf{v}}$ are the versors associated with the $u$ and $v$ axes.

Let us consider the case of a multiple-exposure experiment using different multiple-aperture pupils. The input complex amplitude and the pupil associated with the $k$'th exposure are represented as $A^k(x,y)$ and $\mathsf{P}^k(u,v)$, respectively $(k = 1,2,\ldots,N)$. The input complex amplitudes $A^1, A^2, \ldots, A^N$ are sequentially encoded into the BSO crystal by using a different pupil during each exposure. It should be noted that the number $q$ of apertures of each pupil can vary between exposures.

It is assumed that for any pair of pupils $\mathsf{P}^k$ and $\mathsf{P}^l$, some of their apertures can coincide exactly and the remaining apertures do not overlap at all. Let the functions $a_n^k(u,v)$ and $a_m^l(u,v)$ represent two apertures belonging to the pupils $\mathsf{P}^k$ and $\mathsf{P}^l$ associated with the $k$'th and the $l$'th exposure, respectively, where $n = 1,2,\ldots,q$ and $m = 1,2,\ldots,w$. They are called *common* apertures if $a_n^k(u,v) \equiv a_m^l(u,v)$, and *noncommon* apertures if $a_n^k(u,v) a_m^l(u,v) \equiv 0$.

Furthermore, $a_n^k(u,v) = a(u - u_n^k, v - v_n^k)$, $a_m^l(u,v) = a(u - u_m^l, v - v_m^l)$, where $a(u,v)$ denotes the aperture shape. That is, all the aperture pupils are identical. In the following, circular apertures are considered.

As mentioned above, a photorefractive BSO crystal is employed as the recording medium. These crystals are appropriate for speckle applications where it is necessary to detect in real time any change of the patterns.

The BSO crystal is 3 mm thick and is cut normal to the $\langle \bar{1}10 \rangle$ crystallographic direction. Moreover, the directions $\langle \bar{1}10 \rangle$, $\langle 001 \rangle$, and $\langle 110 \rangle$ coincide with the $X$, $Y$, and $Z$ axes, respectively, along which the linear dimensions are $L_X$, $L_Y$, and $L_Z$. The crystal exhibits the linear electro-optic effect: if a voltage $V$ is applied between the $(\bar{1}10)$ faces, separated by a distance $L_X$, it becomes birefringent due to the external field $E_a = V/L_X$. The intensity distribution projected by the lens $L_1$ in the crystal creates photocharges, which drift due to the external field $E_a$ into the dark regions, where they are trapped. This gives rise to a space-charge field that modulates the refractive index via the linear electro-optic effect.

In the readout step, a collimated plane wave of unit amplitude that is linearly polarized in the $Y$ direction is used. It should be noted that if the readout wavelength $\lambda_R$ coincides with the write-in wavelength, then the readout is destructive and the stored gratings are all progressively erased during this process. This occurs because of the space-charge relaxation (charge redistribution) produced by the reading light. This problem can be partially solved by reading out at a wavelength at which the crystal has low sensitivity. We used a collimated readout beam from a He-Ne laser (10 mW) with $\lambda_R = 633$ nm, which is outside of the spectral sensitivity range of the crystal. Nevertheless, over many cycles, and particularly when using strong beams, this procedure is still destructive.

Then, the reading light transmitted through the crystal is Fourier-transformed by the lens $L_2$ of focal length $f$ and observed on its back focal plane $(\Pi_1)$.

The field amplitude in the Fourier plane, $G(U,V)$, can be expressed as the superposition of Fourier-transformed waves $G^k(U,V)$, $k = 1,2,\ldots,N$, each one representing the complex amplitude associated with an individual exposure:[13]

$$G(U,V) = \sum_{k=1}^{N} G^k(U,V), \tag{1}$$

where $G^k(U,V)$ is the autocorrelation given by

$$G^k(U,V) = \{S^k \otimes (S^k)^*\}(U,V). \tag{2}$$

In this equation $\otimes$ means complex autocorrelation and $S^k(\chi,\zeta)$ is defined as

$$S^k(\chi,\zeta) = P^k\left(-\chi \frac{\lambda_W}{\lambda_R}\frac{Z_C}{f}, -\zeta \frac{\lambda_W}{\lambda_R}\frac{Z_C}{f}\right) T^k \times \left(-\chi \frac{Z_C}{Z_0 f}, -\zeta \frac{Z_C}{Z_0 f}\right), \tag{3}$$

where

$$T^k\left(-\chi\frac{Z_C}{Z_0 f},-\zeta\frac{Z_C}{Z_0 f}\right) = \int A^k(x,y)\exp\left(i\frac{2\pi}{\lambda_R}\frac{Z_C}{Z_0 f}(\chi x+\zeta y)\right)\mathrm{d}x\,\mathrm{d}y. \quad (4)$$

According to Eqs. (1), (2), and (3), the pupil limits the spectral content of the encoded image that contributes to the amplitude field in the Fourier plane. Moreover, it is assumed that $S^k(\chi,\zeta)$ is geometrically similar to $P^k$. Thus, from Eq. (3) it can be inferred that for each exposure the spectral content of each image is gathered into the diffraction spots associated with the respective pupil. Meanwhile the overlapping of the two spectra occurs exclusively in the spots where the two diffraction patterns coincide. In the $U$-$V$ Fourier plane the spectral components of the input $A^k(x,y)$ are concentrated in the regions where

$$\left\{\mathsf{P}^k\left(-\chi\frac{\lambda_W}{\lambda_R}\frac{Z_C}{f},-\zeta\frac{\lambda_W}{\lambda_R}\frac{Z_C}{f}\right) \otimes \mathsf{P}^k\left(-\chi\frac{\lambda_W}{\lambda_R}\frac{Z_C}{f},-\zeta\frac{\lambda_W}{\lambda_R}\frac{Z_C}{f}\right)\right\}(U,V)\neq 0,$$

and the components of $A^l(x,y)$ are located exclusively where

$$\left\{\mathsf{P}^l\left(-\chi\frac{\lambda_W}{\lambda_R}\frac{Z_C}{f},-\zeta\frac{\lambda_W}{\lambda_R}\frac{Z_C}{f}\right) \otimes \mathsf{P}^l\left(-\chi\frac{\lambda_W}{\lambda_R}\frac{Z_C}{f},-\zeta\frac{\lambda_W}{\lambda_R}\frac{Z_C}{f}\right)\right\}(U,V)\neq 0.$$

The main advantages of employing thick photorefractive materials for this implementation are their large information capacity and high diffraction efficiency. Due to the volume nature of the medium, each speckle grain displays information in addition to that observed in two-dimensional media.

It was established in a previous paper[13] that the diffraction efficiency of each speckle grain volume grating behaves like that of a transmission volume hologram. The diffraction efficiency obtained by using coupled-wave theory, taking into account the off-Bragg parameter, predicts a sharp peak at the Bragg angle.[14] When the reading beam is oriented within a small angle around the Bragg angle, the diffraction efficiency is not negligible, but it is clear that such an angular mismatch produces a drop in the diffraction efficiency. This behavior does not represent a disadvantage, because it is possible to obtain diffraction spots with high efficiency by suitably addressing the reconstruction beam. Then, the diffraction efficiency of each speckle grain volume grating can be expressed as

$$\eta=\frac{\kappa^2}{\kappa^2+(\xi/2)^2}\sin^2\left\{L_z\left[\kappa^2+\left(\frac{\xi}{2}\right)^2\right]\right\}, \quad (5)$$

where

$$\kappa=\frac{\pi n\,\Delta n_{ij}^k}{\lambda_R[n^2-\sin^2(\lambda_R d_{ij}^k/\lambda_W\times 2Z_C)]^{1/2}}$$

and the off-Bragg parameter is

$$\xi=\frac{2\pi d_{ij}^k}{Z_C\lambda_W}\frac{\cos(\lambda_R d_{ij}^k/\lambda_W\times 2Z_C)}{[n^2-\sin^2(\lambda_R\cdot d_{ij}^k/\lambda_W\times 2Z_C)]}\Delta\theta_{ij}^k,$$

in which $\Delta\theta_{ij}^k$ is the off-Bragg angle for the fringe system $f_{ij}^k$, $n$ is the refractive index at the wavelength $\lambda_R$, and $\Delta n_{ij}^k$ is the index-grating modulation depth for $f_{ij}^k$.

It is necessary to point out that the diffraction efficiency of the diffraction orders not only depends on the fringe frequency determined by the distance $d_{ij}^k$, but also depends on the orientation of the fringe system $f_{ij}^k$. In our experimental conditions, the diffusion transport of photocharges is negligible and the carrier drift mechanism predominates in developing the index grating. In fact, the external applied field $\mathbf{E}_a$ introduces anisotropic behavior as the grating is built up. That is, the projection of the field $\mathbf{E}_a$ onto the direction of the fringe system $f_{ij}^k$ that modulates the speckle grains establishes the strength of the carrier drift contribution, which in turn develops the index grating. Note that the index-grating modulation depth $\Delta n$ is proportional to the scalar product $\mathbf{E}_a\cdot\mathbf{f}_{ij}^k$. Therefore, the diffraction efficiency depends on this scalar product. In particular, if the two directions are perpendicular to each other ($\alpha_{ij}^k=90$ deg), then the drift mechanism does not contribute to the index-grating formation and the diffraction efficiency is zero.

If several images are multiplexed by using the same multiple-aperture pupil, the encoded speckle distributions are modulated by identical index gratings. Then, in the readout process, the spectral information of all images converges to the same Fourier regions. In contrast, on using a different pupil during each exposure, the loci of the spectral information of the various images in the Fourier plane do not in general coincide. In the observed diffraction patterns corresponding to multiple exposure by using multiple-aperture pupils, some spots of one diffraction pattern coincide exactly in position with some spots of another, whereas the remaining spots do not overlap at all. The appropriate selection of the multiple-aperture pupils allows concentrating the information in chosen regions in the Fourier plane.

An interesting example of multiple exposure by using multiple-aperture pupils is described in Fig. 2. In this case the input images $A^k$ ($k=1,2,\ldots,N$) are sequentially encoded into the crystal by using different pupils $\mathsf{P}^k$. For simplicity, we denote the pupils associated with the first exposure as **A**, with the second exposure as **B**, with the third as **C**, and with the fourth as **D**. In the first row of Fig. 2 these pupils are schematized. In the second row are shown the diffraction patterns obtained from exposure through the pupils. The first diffraction pattern corresponds to one exposure using the pupil **A**. The successive patterns were obtained by multiple exposures by using the pupils **A** and **B**; **A**, **B**, and **C**; and **A**, **B**, **C**, and **D**, respectively. The

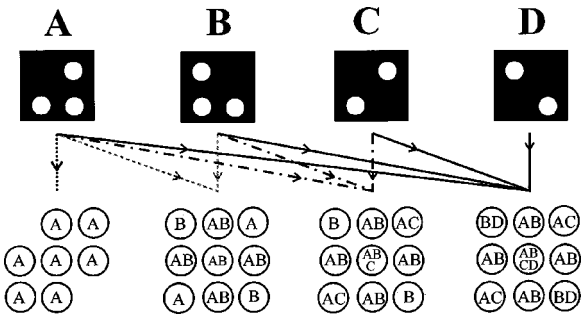


**Fig. 2** Scheme of the pupil arrangement and diffraction patterns corresponding to a single, a double, a triple, and a quadruple exposure by using the pupils schematized above.

capital letter or letters inside each diffraction spot symbolize the information corresponding to each exposure that contributes to that spot.

From the scheme of the diffraction patterns belonging to multiple exposures in Fig. 2, it is apparent that when pairs of pupils are considered there are common and noncommon spots. The pupil arrangements are selected to concentrate in each spot the spectral information corresponding to not more than two exposures. Note that the zero order is always a common spot for arbitrary pupils. The spectral amplitude components for a pair of exposures are added into the common diffraction spots, whereas in the noncommon spots their individual spectra are isolated. In particular, for the four exposures all the diffraction spots contain information about a pair of inputs.

Moreover, it is useful to define the common and noncommon apertures for each pair of pupils. In this context it is assumed that common and noncommon spots can be identified when observing the diffraction patterns corresponding to the multiple-exposure experiment schematized in Fig. 2.

From the diffraction pattern, it is apparent that there is at least one pair of apertures in the pupil **A** that generates in the read out step a pair of lateral diffraction spots that are not obtained when using the pupil **B**. Thus, the light in these (noncommon) spots will carry only spectral information about the input signal $A^1$. A similar conclusion holds when considering the pupil **B** and the input $A^2$. Meanwhile, in the diffraction spots that one pupil diffraction pattern has in common with the other, the spectra of the two encoded images will be overlapped.

## 3 Applications

The experimental setup is shown in Fig. 1. We employed a BSO crystal of dimensions $L_X = L_Y = 10\,\mathrm{mm}$ and $L_Z = 3\,\mathrm{mm}$, with a voltage $V \approx 8\,\mathrm{kV}$ applied between the $(\bar{1}10)$ crystal faces. The distances $Z_0$ and $Z_C$ were 135 and 485 mm, respectively. In the write-in process, light of wavelength $\lambda_W = 514\,\mathrm{nm}$ from an Ar laser was utilized. The incident light intensity onto the crystal was less than 0.4 $\mathrm{mW/cm^2}$. In these experimental conditions, for recording the speckle pattern a time of about one second is needed. In the readout process, we used a plane wave from a He-Ne laser ($\lambda_R = 633\,\mathrm{nm}$), propagating along the $Z$ axis. This reconstruction geometry is the same as used in conventional speckle photography, which implies an off-Bragg readout angle.

As stated above in Eq. (5), the diffraction efficiency of each diffraction spot not only depends on the off-Bragg readout angle, but also depends on the write-in conditions and the crystal parameters. Clearly, the reconstruction can be optimized by Bragg-matching the readout angle. However, making the readout beam incident perpendicularly on the crystal plane (as usual when using a plane recording medium) does not represent a restriction on our setup. Indeed, this arrangement is implemented to display simultaneously all the diffraction spots.

Good tolerance for off-Bragg reconstruction is achieved by using a thin crystal and a small aperture separation. This selection can be done according to the analysis of the diffraction efficiency of the speckle grain volume gratings, as investigated in Ref. 13. From Eq. (5) it can be inferred that the angular half-width of the Bragg peak strongly depends on the writing angle ${\theta_0}_{ij}^{k} = \frac{1}{2} d_{ij}^{k} / Z_C$ and the crystal thickness $L_Z$. In the readout step, when the beam impinges perpendicularly on the crystal plane, this implies an off-Bragg readout angle $\Delta\theta_{ij}^{k} = \theta_{ij}^{k}$, where $\theta_{ij}^{k} = (\lambda_R / \lambda_W)\,{\theta_0}_{ij}^{k}$ is the external Bragg angle for the fringe system $f_{ij}^{k}$. In this readout condition, the diffraction efficiency decreases as $d_{ij}^{k}$ increases. It was shown in Ref. 13 that an increase of the crystal thickness $L_Z$ will produce an increase of the diffraction efficiency. On the contrary, a relatively high off-Bragg condition will produce a lower efficiency as the thickness $L_Z$ increases. Also, it is shown that for $L_Z = 1\,\mathrm{mm}$, the side orders' diffraction efficiency hardly decreases as the aperture separation $d_{ij}^{k}$ increases. In particular, for $d_{ij}^{k} = 14\,\mathrm{mm}$ good diffraction efficiency is observed, which is in accordance with the low angular selectivity corresponding to a thin crystal ($L_Z = 1\,\mathrm{mm}$). A very different situation appears for a thick crystal ($L_Z = 10\,\mathrm{mm}$), and a strong decrease of the efficiency is observed for increasing values of the parameter $d_{ij}^{k}$. In this case, to obtain high efficiency, $d_{ij}^{k}$ must range up to 6 mm, which agrees with the high angular selectivity exhibited by a thick crystal ($L_Z = 10\,\mathrm{mm}$).

A CCD camera and an image processor were employed to record the images. In addition, a red filter prevented the Ar-laser light from impinging on the camera. In our case, circular apertures of diameter $D = 2.65\,\mathrm{mm}$ were used. Then the speckle grains have average depths $S_Z \approx 4\lambda_W (Z_C/D)^2 \approx 85\,\mathrm{mm}$ and $S_X \approx \lambda_W (Z_C/D) \approx 0.1\,\mathrm{mm}$.[11] Note that the speckle depth is larger than the crystal thickness $L_Z$. Thus, it is possible to replace in the write-in process the depth of the speckle by the crystal thickness. The aperture pupils are centered at the vertices of an 8-mm-side-square. As stated in Sec. 2, there is generated in the crystal a multiple system of interferometric fringes in the imaged speckles, whose orientation and frequency are determined by the geometric parameters of the experimental setup.

On using multiple circular apertures, all with the same diameter $D$, the intensity in the Fourier plane consists of circular distributions having all the same spectral width, which is determined by the aperture diameter $D$ of the pu-

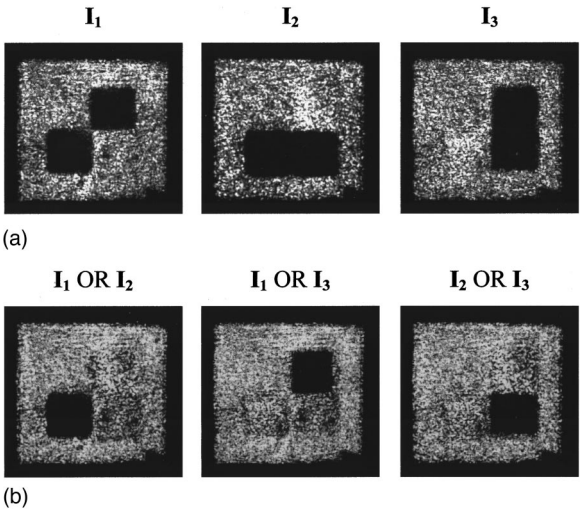


**Fig. 3** (a) Input signals registered in the crystal. (b) Images obtained through a digital operation OR between the input signals shown in (a).

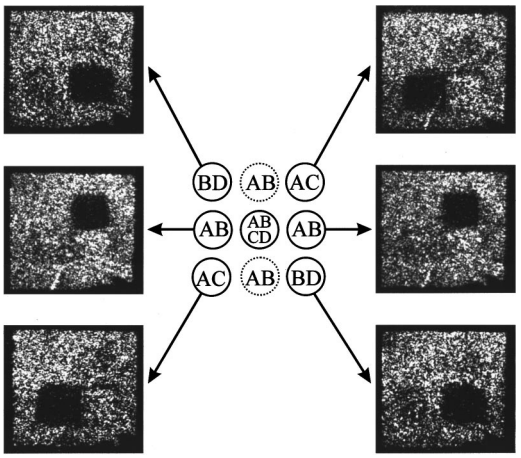


**Fig. 4** Diffraction pattern obtained in the $\Pi_2$ plane and the corresponding images retrieved through filtering out each spot.

pil. As $D$ increases, higher input frequency components will be admitted by the system.

The appropriate selection of multiple-aperture pupils in each exposure allows isolating or combining selectively the spectral information of several multiplexed images into separated zones of the diffraction plane. The spectral amplitude components for each pair of exposures are added into the common diffraction spots, whereas in the noncommon spots their individual spectra are isolated. In this work we present two possible applications of these techniques: to obtain the operation OR between images, and to detect in-plane displacements.

### 3.1 *Image Operations*

One application of this multiple exposure schema is to perform simultaneously the operation OR between each pair of input images. To this purpose it is necessary to select the pupil arrangements, for example as shown in Fig. 2. For this application the transparency is attached to a random diffuser (R in Fig. 1).

In the first row of Fig. 3 are shown three different input signals. In the second row of this figure are shown the output images obtained by digitally realizing the OR operation between each pair of input images.

The Fourier pattern schematized in the middle of Fig. 4 corresponds to the four exposures made with the pupils shown in Fig. 2. In the first exposure the pupil **A** is used. In this case, the image $I_1$ shown in Fig. 3 is registered. Then, for the second exposure, the pupil **B** is used, and the image $I_2$ is registered. Finally, for the third and the four exposures the pupils **C** and **D**, respectively, are used. In both cases, the image $I_3$ is registered. By this procedure, the diffraction spots contain information about a pair of inputs.

In Fig. 4 the dashed circles indicate absent diffraction orders corresponding to vertical apertures ($\alpha_{ij}^{k} \approx 90$ deg). Note that $\Delta n \approx 0$, which implies negligible diffraction efficiency.

In addition, the diffraction efficiency depends strongly on the readout-beam orientation. In this case, the reconstruction can be optimized by Bragg-matching the readout angle. Under this condition the retrieved images can be obtained by using the angular selectivity characteristic of the volume medium.

However, it is possible to reconstruct the stored information in a fixed geometry with the readout beam impinging perpendicularly on the crystal face as in a 2-D medium. In this case, to obtain good performance, it is convenient to employ a thin crystal and a small write-in angle. Under this condition, to retrieve each image a filtering in the Fourier plane is necessary.

In our case, the retrieved images are obtained through properly filtering out the light of each spot in the Fourier plane. To achieve this without cross talk between the images, the diameter of the hole in the filtering mask must coincide with the spot diameter. The image reconstructed through each diffraction spot carries the spectral information for a single pair of exposures. The information stored in each spot is reconstructed by means of lens $L_3$ at the $\Pi_2$ plane. The image reconstructed correspond to the operation OR among the input images $I_1$, $I_2$, and $I_3$. This is confirmed by comparing the images of Fig. 3 with the images reconstructed through the different diffraction spots. Rather low spatial resolution of the retrieved images is observed, mainly because only some spectral components (those admitted by the pupils) contribute to the images.

In summary, this procedure allows an alternative implementation of the operation OR between input images.

### 3.2 *In-Plane Displacements*

In speckle photography some advantage can be gained by utilizing different multiple-aperture pupils. As discussed above, the use of different pupils allows one to isolate or to combine selectively the spectral information of several multiplexed images in separated regions of the diffraction plane. This selection allows storing several in-plane displacements.

Examples of interferometric fringes achieved by multiplexing one, two, three, and four modulated speckle distributions are depicted in Figs. 5(a), 5(b), 5(c), and 5(d), respectively. The four images were recorded according to the scheme depicted in Fig. 2. Between the first and the second

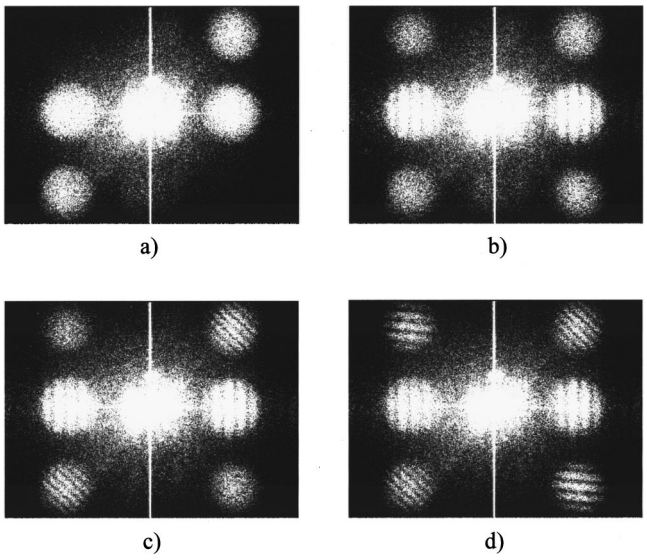


**Fig. 5** (a) Single-exposed, (b) double-exposed, (c) triple-exposed, and (d) quadruple-exposed specklegrams for several in-plane displacements between images recorded through the pupils schematized in Fig. 2.

exposure, a horizontal 80-$\mu$m displacement of the diffuser was made. Afterwards, a vertical 90-$\mu$m displacement was made between the second and the third exposure. Thus, the third image was both horizontally and vertically displaced with respect to the first image. In the third and the fourth exposure, the diffuser was displaced in the same magnitude with respect to the first exposure; that is, no relative displacement existed between the last two images.

The registers displayed in Fig. 5 correspond to the plane $\Pi_1$ in the setup depicted in Fig. 1.

In Fig. 5(a) the fringes do not appear at the diffraction spots, because only one specklegram is registered. In Fig. 5(b) the horizontal spots exhibit fringes. The common apertures of the pupils **A** and **B** are responsible for the diffracted light in these spots. Notice that the fringe orientation corresponds to the horizontal displacement between the first and the second image. Fringes do not appear in the diagonal spots, because only the light diffracted by the pupil **A** or **B** goes there. Nevertheless, there are noncommon aperture pairs in the pupils **A** and **B** responsible for that spot's formation. In Fig. 5(c) a fringe system appears only in a pair of diagonal spots. The appearance of fringes in these spots can be interpreted by considering the fact that the spectra of the first and the third image are overlapped there. The period and orientation of the fringes correspond to the relative displacement between the first and the third image. The third and the fourth image were equally displaced with respect to the first. Then, as a consequence of the overlapping of the spectral components of the second and the fourth image, a new system of fringes appears exclusively in the other diagonal spots. In fact, these (horizontal) fringes refer to the relative vertical displacement between the respective images. The remaining spots do not change on adding the fourth image.

Finally, in the central spot the spectra of the three images are overlapped. Furthermore, a rather complex spatial modulation appears, because horizontal, vertical, and diagonal fringes are also overlapped there.

In summary, in this experiment the fringe-modulated diffraction spots correspond to three independent double-exposed specklegrams. These fringes have optimum visibility and correspond to different relative displacements. In addition, only four recording steps are needed, and the relative displacements between nonconsecutive images are obtained.

## 4 Conclusions

An alternative image-multiplexing technique based on image modulation through speckle patterns, by using different multiple aperture pupils for recording, has been presented. The use of a different pupil mask for each exposure has a definite advantage in that it allows concentrating the spectral components of individual images into isolated spots in the Fourier plane. Image multiplexing through a suitable selection of multiple-aperture pupils allows retrieving the overlap between each pair of input images.

A thick photorefractive BSO crystal is used for the proposed applications because of its real-time response and large storage capability. Notice that the volume medium employed raises the possibility of exploiting its inherent angular selectivity either to retrieve one spot each time or to reconstruct all the spots simultaneously in a fixed geometry with good diffraction efficiency through an appropriate selection of the geometric parameters of the pupil mask.

In this paper, two applications were discussed. In the field of image processing, the image binary operation OR is carried out. Another application is to storing in the crystal the information belonging to several in-plane displacements. Conventional speckle photography requires three consecutive steps: recording, development, and readout. In contrast, all these steps occur simultaneously in the BSO crystal, which has high sensitivity and a short time constant for recording and erasure.

We have restricted ourselves to demonstrating the application of speckle photography to uniform in-plane displacements. Nevertheless, it is possible to implement the technique for a pointwise displacement analysis using multiple exposures, or for whole-body displacements. In this case, different sets of contour fringes, each one depicting equal displacements in a given direction, could be observed when filtering the specklegrams.

### *Acknowledgments*

This research was performed under the auspices of the CONICET, PIP 4710 (Argentina) and Facultad de Ingeniería, Universidad Nacional de La Plata (Argentina). L. Angel also acknowledges support from the Instituto Colombiano para el Desarrollo de la Ciencia y la Tecnología (Colombia).

### *References*

1. E. N. Leith and J. Upatnieks, ''Wavefront reconstruction with diffuser illumination and three dimensional objects,'' *J. Opt. Soc. Am.* **54**, 1295 (1964).
2. H. J. Caufield, ''Wavefront multiplexing by holography,'' *Appl. Opt.* **9**, 1218–1219 (1970).
3. F. H. Mok, ''Angle-multiplexed storage of 5000 holograms in lithium niobate,'' *Opt. Lett.* **18**, 915–917 (1993).
4. P. Huignard and P. Günter, Eds., *Photorefractive Materials and their Applications II*, Springer-Verlag, Berlin (1989).

5. H. J. Tiziani, K. Leonhardt, and J. Klenk, ''Real-time displacement and tilt analysis by a speckle technique using $Bi_{12}SiO_{20}$ crystals,'' *Opt. Commun.* **34**, 327–331 (1980).
6. H. J. Tiziani and J. Klenk, ''Vibration analysis by speckle techniques in real time,'' *Appl. Opt.* **20**, 1467–1470 (1981).
7. K. Nakagawa and T. Minemoto, ''Improvement of Young's fringes in speckle photography by use of a BSO-PROM device,'' *Opt. Commun.* **70**, 288–292 (1989).
8. K. Nakagawa, T. Takatsuji, and T. Minemoto, ''Measurement of the displacement distribution by speckle photography using a BSO crystal,'' *Opt. Commun.* **76**, 206–212 (1990).
9. K. Nakagawa and T. Minemoto, ''Readout properties of the speckle-gram recorded in photorefractive $Bi_{12}SiO_{20}$ crystal,'' *Appl. Opt.* **30**, 2386–2392 (1991).
10. R. Tripathi, G. S. Pati, A. Kumar, and K. Singh, ''In-plane displacement measurement using a photorefractive speckle correlator,'' *Opt. Commun.* **149**, 355–365 (1998).
11. M. Francon, *La Granularité Laser (Speckle) et Ses Applications en Optique*, Mason, Paris (1977).
12. J. C. Dainty, Ed., *Laser Speckle and Related Phenomena*, Springer-Verlag, Berlin (1975).
13. M. Tebaldi, L. Angel, M. C. Lasprilla, and N. Bolognini, ''Image multiplexing by speckle in a BSO crystal,'' *Opt. Commun.* **155**, 342–350 (1998).
14. H. Kogelnik, ''Coupled wave theory for thick hologram gratings,'' *Bell Syst. Tech. J.* **48**, 2909–2247 (1969).

**Myrian Tebaldi** received her MS and PhD degrees in physics from the University of La Plata, Argentina, in 1994 and 1998, respectively. She teaches physics in the Facultly of Engineering of the University of La Plata and is a researcher at the Optical Research Center (CIOp), La Plata. Her current research interests include real-time image processing with photorefractive crystals and speckle techniques.

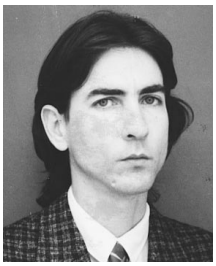

**Luciano Angel Toro** received his MS degree in physics from the Department of Physics of the Universidad de Antioquia, Colombia, in 1991. He is currently an associate professor at Universidad EAFIT, Colombia, and is a PhD candidate at the Universidad Nacional de La Plata, Argentina. He is involved in optical processing using photorefractive materials and digital techniques at Centro de Investigaciones Opticas (CIOp), Argentina.

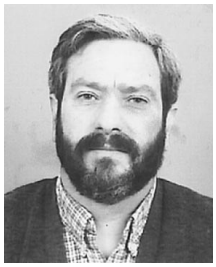

**Marcelo Trivi** received his MS and PhD degrees in physics from the University of La Plata, Argentina, in 1979 and 1986, respectively. In 1982 he joined the Optics Group at the Optical Research Center (CIOp), La Plata, and since 1988 has been a researcher with the Buenos Aires Research Council (CICPBA), Argentina. He is currently a professor in the Faculty of Engineering, National University of La Plata. He spent four years at the Istituto Nazionale di Ottica, Florence, Italy, under a Fellowship of the International Centre for Theoretical Physics, Trieste, Italy. He was an invited professor at the University of Antioquia, Medellin, Colombia. His current research interests include optical processing, TV holography, dynamic speckle, and optical metrology.

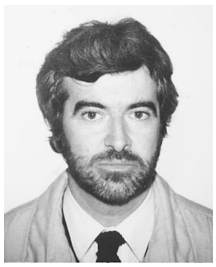

**Néstor Bolognini** received his PhD in physics from the Universidad Nacional de La Plata, Argentina, in 1981. He joined the Centro de Investigaciones Opticas (CIOp) in La Plata in 1977. He did research at the University of Stuttgart and the Universidad Autónoma de Madrid. His research activities have included speckle techniques, holography, and Fourier optics. He is involved in image processing using photorefractive materials and is currently a researcher of CONICET (Nacional Research Council of Argentina), a professor of physics at Universidad Nacional de La Plata, and a PhD thesis adviser.